Tellus (2008), 60A, 557–569
Printed in Singapore.

TELLUS

Climatological properties of summertime extra-tropical storm tracks in the Northern Hemisphere

By MICHEL DOS SANTOS MESQUITA[1,3]*, NILS GUNNAR KVAMSTØ[1,2], ASGEIR SORTEBERG[2] and DAVID E. ATKINSON[3], [1]*Geophysical Institute, University of Bergen, Allégaten 70, N-5007 Bergen, Norway;* [2]*Bjerknes Centre for Climate Research, University of Bergen, Allégaten 55, N-5007, Norway;* [3]*International Arctic Research Center, University of Alaska Fairbanks, 930 Koyukuk Drive, Fairbanks, Alaska 99775, USA*

(Manuscript received 26 April 2007; in final form 20 December 2007)

ABSTRACT

This paper presents climatological properties of Northern Hemisphere summer extratropical storm tracks using data extracted from an existing, relative-vorticity-based storm database. This database was constructed using the NCEP-NCAR 'Reanalysis I' data set from 1948 to 2002. Results contrasting summer and winter patterns for several storm parameters indicated general similarity at the largest scales, including the prominent track corridors of the middle latitude ocean regions and the mid-continental and east coast genesis zones. Variations between seasons generally consisted of differences in the strength and position of these major features. Several results underscored by this study are: summer storms have longer life-spans than their winter counterparts; the Atlantic track corridor in summer is more tightly confined over northern Europe, whereas in winter it is more diffuse; summertime Atlantic storms are found to be slightly weaker but more numerous than their Pacific counterparts; Pacific storm counts exhibit a large drop from winter to summer that is not observed in the Atlantic; and summer storms appear to be related to the summer NAM, PDO and NAO.

1. Introduction

Numerous studies have been conducted that focus on understanding and describing the behaviour of winter storm tracks (see for example, Cai and van der Dool, 1991; Chang and Orlanski, 1993; Serreze et al., 1993; Lambert, 1996; Serreze et al., 1997; Simmonds and Keay, 2000; Graham and Diaz, 2001; Gulev et al., 2001; Byrkjedal, 2002; Chang et al., 2002; Chang and Fu, 2002; Hoskins and Hodges, 2002; Zolina and Gulev, 2002; Anderson et al., 2003; Hodges et al., 2003; Simmonds et al., 2003; Chang, 2004; Pinto et al., 2005; Sorteberg et al., 2005; Mailier et al., 2006. By contrast, the summer season has seen relatively little research activity (Reed and Kunkel, 1960; Whittaker and Horn, 1984; Serreze et al., 1993, 1997; Norris, 2000; Simmonds and Keay, 2002; Zhang et al., 2004). This stems from the basic tenet that winter storms are more frequent and vigorous, tend to cause more damage, and thus have garnered greater attention.

Summer storms, however, also have potential for serious damage. One example of a powerful summer extra-tropical storm occurred on August 13–14, 1979, as reported by Lamb (1991). A yacht race was going on in Great Britain during that time. The storm overwhelmed race participants, leaving 24 yachts abandoned and 15 crew members drowned. Other examples include the storm of July 29, 1956 (Lamb, 1991), which also sank a British tall ship (the *Moyana*) returning from the first International Tall Ships race, and a severe storm in August, 2000. Indeed, in 1588 the damaged and retreating Spanish Armada sustained further heavy damage when it sailed into a severe summer storm off of Ireland.

The damage potential of summer season cyclones underscores our interest to present a comprehensive picture of their climatology and variability. In fact, from a European perspective it can be argued that, even though summer storms may not be as intense as those in winter, it is the summer storms that reach western/northern Europe, and so are as likely to be problematic as winter storms. In addition to better understand the damage threat, a good description of summer season processes can support other research efforts by providing greater insight concerning the interplay between background flow and lower boundary properties and it can aid in GCM verification work. The objectives of this paper, therefore, are to:

*Corresponding author.
e-mail: michel@iarc.uaf.edu
DOI: 10.1111/j.1600-0870.2008.00305.x

(a) present a detailed summer season storm track climatology for four selected storm parameters (cyclogenesis density, track density, feature intensity, and event lifetime),

(b) contrast this with a similar climatology determined for the winter season,

(c) examine temporal trends in the storm parameters, and

(d) assess the strength of relationships between observed patterns and major Northern Hemisphere atmospheric modes of variability.

Climatologies presented in this paper are based on a previously constructed database of storm characteristics (Sorteberg, 2004, personal communication). The manner by which a 'storm' is defined and tracked is not an entirely objective exercise. For this reason a brief discussion of the various methods, as well as a justification for the selection employed here, is also provided. In general, a variety of storm tracking techniques have been developed, ranging from manual counting methods used in decades past (e.g. Keegan, 1958; Reed and Kunkel, 1960; Lydolph, 1977; Whittaker and Horn, 1984) to more modern computer-based ('automated' or 'objective') algorithms (Murray and Simmonds, 1991; Jones and Simmonds, 1993; Serreze et al., 1993; Hodges, 1995; Sinclair, 1995). Different variables, corresponding to different storm 'definitions', have also been used to identify and count cyclones.

Some of the previous summer studies were based on manual tracking, or on the MSLP to track the storms or they were region limited. For example, the Reed and Kunkel (1960) data set was based on historical map charts and manual tracking. Whittaker and Horn (1984) performed their analysis manually and they worked with July data for the summer season. Serreze et al. (1993, 1997) worked with an algorithm based on MSLP to track the storms. Serreze et al. (1997) worked with what they called a 'warm season', that is, an extended summer from April through September. Norris (2000) focused on the North Pacific and the storm track is diagnosed by the root-mean-squared daily vertical velocity at 500 mb. Simmonds and Keay (2002) main focus was to determine the surface fluxes of momentum and mechanical energy. Zhang et al. (2004) used the MSLP as the tracking variable applied to the Arctic region. The authors mentioned that their tracking produced artificial results as well, for example, regions with high topography (e.g. Greenland) gave artificially high cyclone frequencies because of negative biases introduced by the extrapolation of pressure to sea level. Even though the authors had used a similar algorithm to that of Serreze et al. (1997), with some modifications, they argued that some inconsistencies were found due to the different definitions of cyclone trajectory count and cyclone centre count as well as to the domain area.

In this paper, we use relative vorticity at 850 hPa over the entire Northern Hemisphere as the tracking variable. The method employed provides a range of descriptive tracking variables. We further contrast the summer distribution of those with the winter situation and relate their variability to the large-scale climatological patterns.

There are two main categories of automated approaches. The first involves band-pass filtering (e.g. Blackmon, 1976; Blackmon et al., 1977). This approach diagnoses storm track activity by determining statistics associated with pre-defined synoptic timescales, such as, the variance in a frequency band. A primary limitation with band-pass filters is that, although they highlight spatial patterns associated with various timescales (synoptic in this case), these patterns are not always necessarily related to storms (Anderson et al., 2003). This is partly because a narrow band only emphasizes a particular timescale whereas cyclones may have different timescales associated with their lifecycles. Several properties of the band-pass approach have been thoroughly reviewed by Chang et al. (2002).

The second approach is the method of 'feature tracking', in which a definition for a 'cyclone' is adopted and objectively applied to gridded fields of atmospheric variables. In this manner discrete cyclones are identified and tracked. While the most commonly used feature tracking method is that based on Mean Sea Level Pressure (MSLP) (Serreze et al., 1993), in the present paper a feature tracking algorithm which instead identifies and tracks cyclones using relative vorticity (ζ), developed by Hodges (1994, 1995, 1996, 1999), is employed. ζ has several appealing properties which motivated its selection, including:

(i) it identifies systems earlier in their life cycle
(ii) it is directly related to the wind speed
(iii) it is not influenced by strong background flows occurring at large spatial scales (Barry and Carleton, 2001; Hoskins and Hodges, 2002).

It must be noted that, although we have argued for one method versus another, thinking in absolute terms of trying to pick a 'best' method is not profitable because the act of precisely defining a 'storm' can possess a certain degree of subjectivity, rendering logical bases for justification somewhat circular. In fact there are many procedures for storm track identification (Keegan, 1958; Reed and Kunkel, 1960; Reitan, 1974; Zishka and Smith, 1980; Whittaker and Horn, 1981; Bell and Bosart, 1989; Serreze et al., 1993; Lambert, 1996; Hoskins and Hodges, 2002), rendering an absolute, quantitative comparison difficult. The differences between storm track climatologies may arise due to methodology and the tracking variable employed (e.g. Serreze et al., 1997; Gulev et al., 2001; Hoskins and Hodges, 2002; Zhang et al., 2004). In order to directly test the potential influence of the data set on the results generated with a given tracking method, Hodges et al. (2003), using different re-analysis data sets, demonstrated that only negligible disagreements are introduced in the Northern Hemisphere lower troposphere. However, this is not the case for the Southern Hemisphere, in which 'agreement is found to be generally less consistent in the lower troposphere with significant differences in both track density and mean intensity' (Hodges et al., 2003).

Turner et al. (1998) show that the type of methodology selected for identification and tracking may produce significantly different results with important consequences for derivative studies (e.g. poleward energy transfer). A case in point may be made by contrasting work by Jones and Simmonds (1993) with that of Sinclair (1994), both of which presented methodologies to identify and track systems in the Antarctic. Jones and Simmonds (1993) suggest that the zone of circumpolar trough (55-65S in their paper) was one of minimum cyclone density, cyclogenesis, and cyclolysis. This is in disagreement with what Sinclair (1994, 1995), who used a geostrophic-vorticity-based tracking algorithm, and other studies from the 1960s (see Turner et al., 1998), that depressions generally form and develop within midlatitudes and then move eastward and poleward. Besides that, Sinclair suggested that this view was also consistent with earlier satellite climatologies and general synoptic experience (Turner et al., 1998).

In addition, Leonard et al. (1999) compared results obtained using three different tracking methods with storm tracks identified on satellite imagery in the Antarctic. The algorithms analysed were: Terry and Atlas (1996), which locates the innermost closed contour in a low pressure system using MSLP; König et al. (1993), which does a grid point search to find a minimum in the MSLP field; and Murray and Simmonds (1991), which locates maxima in the curvature of a bi-cubic spline fitted to MSLP field, it also tracks both open and closed lows. The three models present differences in both the number of storms and their locations. The authors found that the Murray and Simmonds (1991) identifies more low-pressure centres, whereas Terry and Atlas (1996) finds the least. The Atlas and Terry and Konig et al. schemes found more lows at high latitudes as a result of using data on a latitude/longitude grid (Leonard et al., 1999). The authors suggest that a model should be chosen based on the needs of the analyst, or as they pointed out that when carrying out an intercomparison of depression tracking schemes great care must be taken not to draw misleading conclusions on the merits and value of a particular scheme, since different users of a software may have different requirements (Leonard et al., 1999).

Pinto et al. (2005) have also pointed out the influence of spatial and temporal choices for storm track detection. They used a tracking method originally created for the Southern Hemisphere (Murray and Simmonds, 1991; Simmonds et al., 1999) and tuned it for the Northern Hemisphere. They worked with the MSLP and the quasi-geostrophic relative vorticity (determined from the Laplacian of the pressure) fields. The authors concluded that lowering of the spatial and temporal resolution of the input data from full resolution (T62/06 h to T42/12 h in their study) actually decreased the cyclone track density and cyclone counts. In addition to that, reducing the temporal resolution alone may contribute to a decrease in the number of fast moving systems. Lowering spatial resolution alone may reduce the number of weak cyclones.

The layout of the paper is as follows; Section 2 details the data and methods used. Section 3 presents results, including: (1) description of the main features of the climatology of the extra-tropical summer storms in the Northern Hemisphere; (2) a comparison between summer and winter climatologies; (3) storm parameter trends in the Atlantic and Pacific and (4) storm track variability and its relation to the major modes of atmospheric large-scale variability.

Although plots for the entire Northern Hemisphere are presented, discussion will concentrate largely on the main storm track and cyclogenesis regions of the mid-latitudes/subarctic zone.

2. Data and Methodology

The tracking algorithm developed by Hodges (1994, 1995, 1996, 1999) is employed here to build the cyclone event database. This algorithm identifies feature points using the maxima in the relative vorticity fields, and it links successive time steps by means of a cost function. Then, an estimate of the cyclone descriptive statistics is obtained on a seasonal basis. Cyclones of short duration (<2 d) or which were nearly stationary [$<5^\circ$ travel along a great circle (Hodges, 1999; Hodges et al., 2003)] were removed.

The 850-hPa relative vorticity fields used came from the NCEP/NCAR reanalysis I, provided by the NOAA-CIRES Climate Diagnostics Center (Kalnay et al., 1996; Kistler et al., 2001). Specifically, 6-hourly 850-hPa relative vorticity, calculated from the wind components during the period 1948–2002, was used. We have chosen to work with the NCEP Reanalysis data set from 1948(49) to 2002 even though this period of time includes pre-satellite data, and that there were fewer upper-air data for the first decade, 1948–1957, (Kistler et al., 2001). Other papers related to storm tracking have also worked with the NCEP Reanalysis data for the same period of time as in: Zhang et al. (2004), who worked with data from 1948 to 2002; Sorteberg et al. (2005), who worked with data from 1948 to 2002; Mailier et al. (2006), whose data was from 1950 to 2003, and Sorteberg and Walsh (2008), who worked with the period from 1949 to 2002.

Local positive relative vorticity extremes with values greater than $1 \times 10^{-5}\,\mathrm{s}^{-1}$ were identified and the extremes for two consecutive time steps were linked together using the image processing technique of Salari and Sethi (1990) that is based on a cost-function which evaluates track smoothness in terms of changes in direction and speed (Hodges, 1995, 1996). The technique has been generalized to a spherical domain (Hodges, 1995), which obviates the need to use projections and reduces geometric bias (Zolina and Gulev, 2002). This also allows the analysis of large spherical regions to be performed. Some data pre-conditioning was applied. Planetary-scale circulation with wave numbers fewer than 7 were removed from the vorticity field prior to the tracking method. In contrast to the MSLP, this spectral cut-off does not make any significant change to the results since the planetary scales are relatively weak in the vorticity fields relative to the anomalies (Hodges et al., 2003; Sorteberg and Walsh, 2006). This filtering process was based on the method by Anderson et al. (2003).

The described tracking algorithm returns a set of descriptive parameters for each cyclone trajectory (referred to as 'storm' hereafter). These are statistically aggregated into the seasonal data sets employed for this study. The track density statistics are scaled to number density per month per unit area, where the unit area is 10^6 km^2, which is approximately equivalent to 5° spherical cap (Hodges et al., 2003). The following four parameters were utilized for this work (see Hodges, 1996, for the calculation method):

(i) *Genesis density:* Density of starting points for storm trajectories per season (10^6 km^2 season)$^{-1}$.

(ii) *Track density:* Density of storms traversing an area per season (10^6 km^2 season)$^{-1}$. One point from each storm track that is closest to the estimation point constitutes a single event datum.

(iii) *Intensity:* Mean intensity (vortex depth in s^{-1}) of the storm (per 10^6 km^2 estimation region).

(iv) *Mean lifetime:* Mean lifespan (in days) of the storm in a region (per 10^6 km^2 estimation region).

The major modes of atmospheric large-scale variability used were obtained from:

(1) *The summer Northern Annular Mode (NAM):* The NAM data set (Ogi et al., 2004) was obtained from Ogi's website at: *http://wwwoa.ees.hokudai.ac.jp/svnam/SV − NAM − 48 − 05.txt*.

(2) *The Pacific Decadal Oscillation (PDO):* PDO index data (Zhang et al., 1997) obtained from the Joint Institute for the Study of the Atmosphere and Ocean, JISAO, Seattle, USA, at *http://jisao.washington.edu/pdo/PDO.latest*.

(3) *The North Atlantic Oscillation (NAO):* The NAO Index Data was provided by the Climate Analysis Section, NCAR, Boulder, USA, Hurrell (1995).

3. RESULTS

The results presented here will centre around analyses conducted on the four storm descriptive parameters listed above, and will include general climatology patterns, linear trends for the 1948–2002 period, variability, and a comparison between summer and winter patterns.

3.1. Climatology

The strongest control on summer (JJA, Fig. 1a) and winter (DJF, Fig. 2a) cyclogenesis is associated with orographic features and baroclinic zones. The location of summer cyclogenesis is further north as compared to winter. The largest Northern Hemisphere maximum (JJA) is observed on the lee side of the Rocky Mountains. This region of topographically enhanced vorticity comprises a large area stretching from the southern United States up into Canada. The Rocky Mountains, oriented transverse to the background flow, generate enhanced cyclonic activity on its lee side due to the conservation of potential vorticity (Bluestein, 1993; Holton, 2004). The second major cyclogenesis zone in the Northern Hemisphere is the smaller region located in northeast China/central Siberia, south of Lake Baikal (Fig. 1a). This region is a zone of strong baroclinicity, feeding off of a maritime flow from the Sea of Japan and the northwest Pacific.

Secondary genesis density maxima are found over northern Europe/Eurasia, the North Pacific, and the North Atlantic/North American eastern seaboard regions. These baroclinic zones are present due to polar front location or by the juxtaposition of the warm continental mass and cool ocean that act to maintain a strong thermal gradient. However, we do find areas with significant baroclinicity which are not associated with high cyclogenesis density, particularly in northeast Siberia. In contrast to our finding here, Serreze et al. (2000) found a maximum in cyclogenesis in the lee of the Verkhoyansk range. The reason for this contradiction is not clear. However, it may be related to the use of vorticity in the 850mb level instead of MSLP, which Serreze et al. (2000) used. Or it could be related to other differences in the tracking methodology, such as the removal of cyclone tracks of short duration (<2 d) or nearly stationary (<5 degree travel along a great circle) cyclones.

Two major zones of storm density maxima are observed over the North Atlantic/eastern North America and the North Pacific (Fig. 1b). These define the most prominent storm tracks in the Northern Hemisphere.

The North Atlantic track, and the region of highest summer cyclone density counts, starts in the eastern part of Canada in the lee of Rocky Mountains and extends east to the ocean then east–northeast across the North Atlantic to reach Iceland/England (Fig. 1b).

The North Pacific track, with slightly less cyclone density than the North Atlantic track, extends northeastward from northeast Asia across the North Pacific over to the Gulf of Alaska (Fig. 1b).

Secondary regions of lower track densities are found over all of northern Eurasia extending to the pole, eastern Asia, and northern Canada extending over the pole.

The climatology of the storm intensity (Fig. 1c) exhibits a feature density similar to many of the same features observed in the track density field (Fig. 1b). The areas with deepest vortices are found south of Greenland and Iceland and in the Aleutian region. High intensities are also found south of Japan, although this area is outside the main track corridor.

A mean storm life span of approximately 6 d is observed in the zones of storm track maxima (Fig. 1d). Relatively long-lived storms are observed over the central Arctic region. It was found that most summer storms—55%—last 5–7 d. Another 40% of storms last from 2 to 4 d and long-lived storms, those

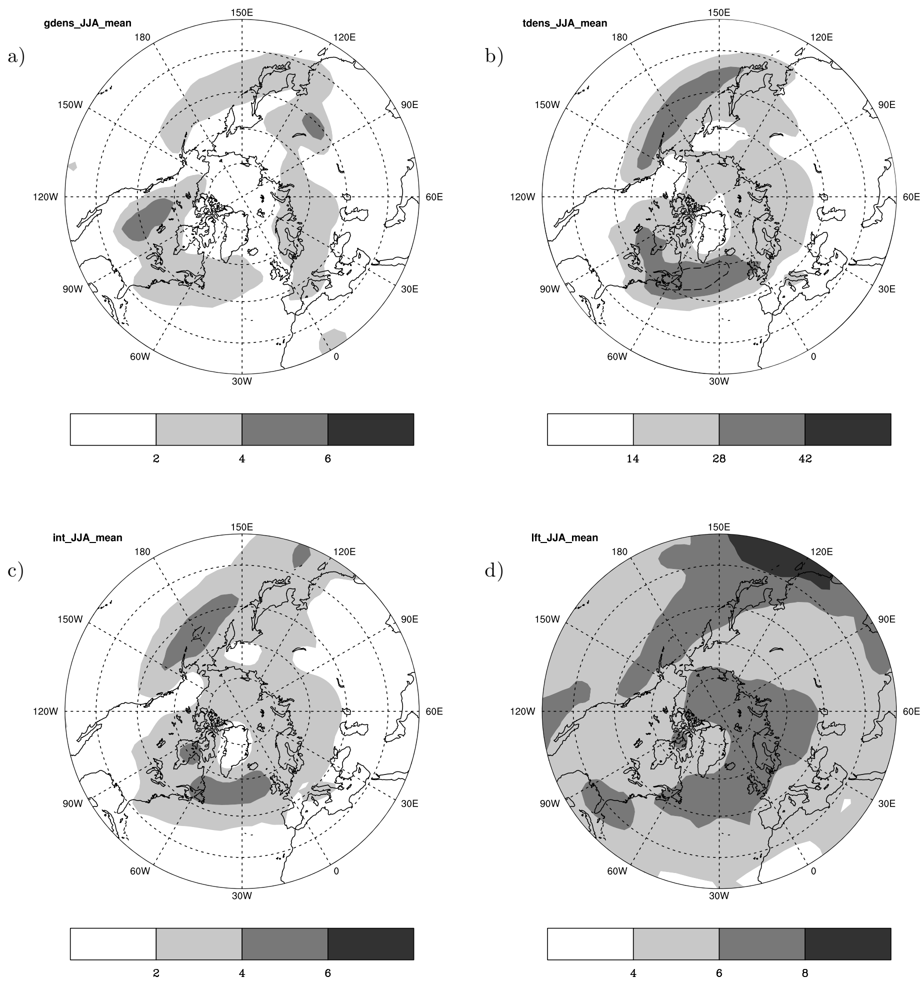

Fig. 1. Climatology of summer (JJA) storm tracks in the Northern Hemisphere from 1948 to 2002: (a) The genesis density (10^6 km^2 season)$^{-1}$; (b) The track density (10^6 km^2 season)$^{-1}$. To better indicate the larger number of storms in the Atlantic a contour line at 36 storms (10^6 km^2 season)$^{-1}$ was added; (c) The track intensity (10^{-5} s^{-1}). Added contour line: 4.5 (10^{-5} s^{-1}); (d) The mean lifetime (d).

with lifetimes exceeding 7 d, constitute 5% of the summer storms observed in the Northern Hemisphere.

3.2. *Comparison between summer and winter*

In this subsection, the climatology of the difference between summer and winter storms is discussed with respect to the four parameters. Raw values for winter are presented for reference (Fig. 2). The difference results, defined as winter values minus summer values (Fig. 3), form the main focus of discussion.

Wintertime genesis patterns are similar to those found in summer, with localized cores of high activity (Fig. 3a). This is in keeping with the stronger baroclinic zones associated with the more intense and southerly positioned polar front and the stronger continental/maritime thermal gradients of the winter season.

The difference between summer and winter track densities (Fig. 3b) is manifested as generally lower densities during summer in the (low) mid-latitudes, where we find the climatological winter maxima (storm track). Further north, however, summer genesis densities are greater, in particular over the Pacific, North-Atlantic and the northeastern parts of the North-American and Asian continents. This indicates both a weakening and northward shift of the Northern Hemisphere storm track during summer.

The northward shift of the Atlantic summer storm track takes place in the western part, while in the eastern (exit) part, close to the British Isles and the south Norwegian coast, the summer track density does not shift but instead appears more concentrated. The wider winter storm track exit region curves cyclonically and is more longitudinally directed along the Norwegian coast into the Barents Sea. However, in summer, the storm track exit region is more concentrated, oriented east–west, and situated further south in the United Kingdom/Scandinavia region.

In Asia, the most enhanced features in the summertime are found over parts of the Russian Federation, most of China, the northern part of Japan and over the Sea of Okhotsk. The values

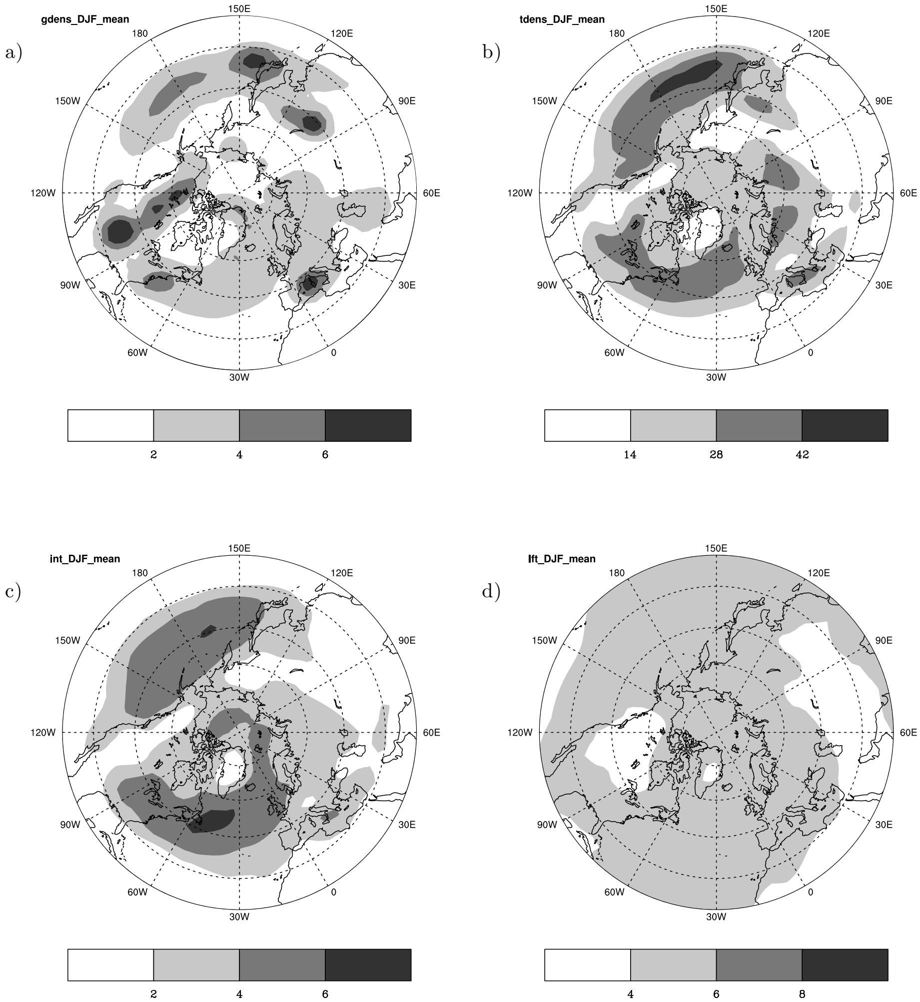

Fig. 2. Climatology of winter (DJF) storm tracks in the Northern Hemisphere from 1949 to 2002: (a) The genesis density (10^6 km^2 season)$^{-1}$; (b) The track density (10^6 km^2 season)$^{-1}$; (c) The track intensity (10^{-5} s^{-1}); (d) The mean lifetime (d).

over these areas are up to even six events per season more than during winter. In the North Pacific, especially over the Bering Sea, the range of the number of tracks is on the order of 2–5 more storms (10^6 km^2 season)$^{-1}$ (Fig. 3b).

The mean intensity is stronger during winter in most areas (Fig. 3c). The exceptions are regions close to the Rocky Mountains, over Hudson Bay, Foxe Basin, Hudson Strait and parts of Québec where summer storms are more intense on average. In most of the North Atlantic, the intensity of winter storms is approximately 40% greater than summer.

However, over Europe, mean intensity is only slightly larger in winter than in the summer season. In Asia, the storm intensity in the summer is higher in most of the eastern parts, such as China, Mongolia and parts of the Russian Federation.

Mean summer storm lifetime exceeds winter storm lifetime over almost the entirety of the Northern Hemisphere storm track regions (Fig. 3d). In some areas, such as over England and parts of Scandinavia, summer storms lifespan exceeds winter storm lifespan by 2 or more days. Zhang et al. (2004) found similar results though their work was confined to the Arctic region.

In North America, the storms are up to 1.5 d longer in summer. This is also similar in the North Atlantic. This difference is smaller through most parts of Asia and the Russian Federation, with values up to around 1.25 d, and larger the North Pacific, particularly over the Gulf of Alaska and on the west coast of Canada, where summer storms last up to 2.25 d longer. Over the Arctic region summer storms last up to 2 d longer than in winter.

3.3. *Trends*

Long-term rates of change are presented for two regions in the Atlantic (identified as 'A1' and 'A2', Fig. 4) and one in the Pacific (identified as 'P', Fig. 4). Reasons for selecting them are as follows: A1—important cyclogenesis and primary track zone;

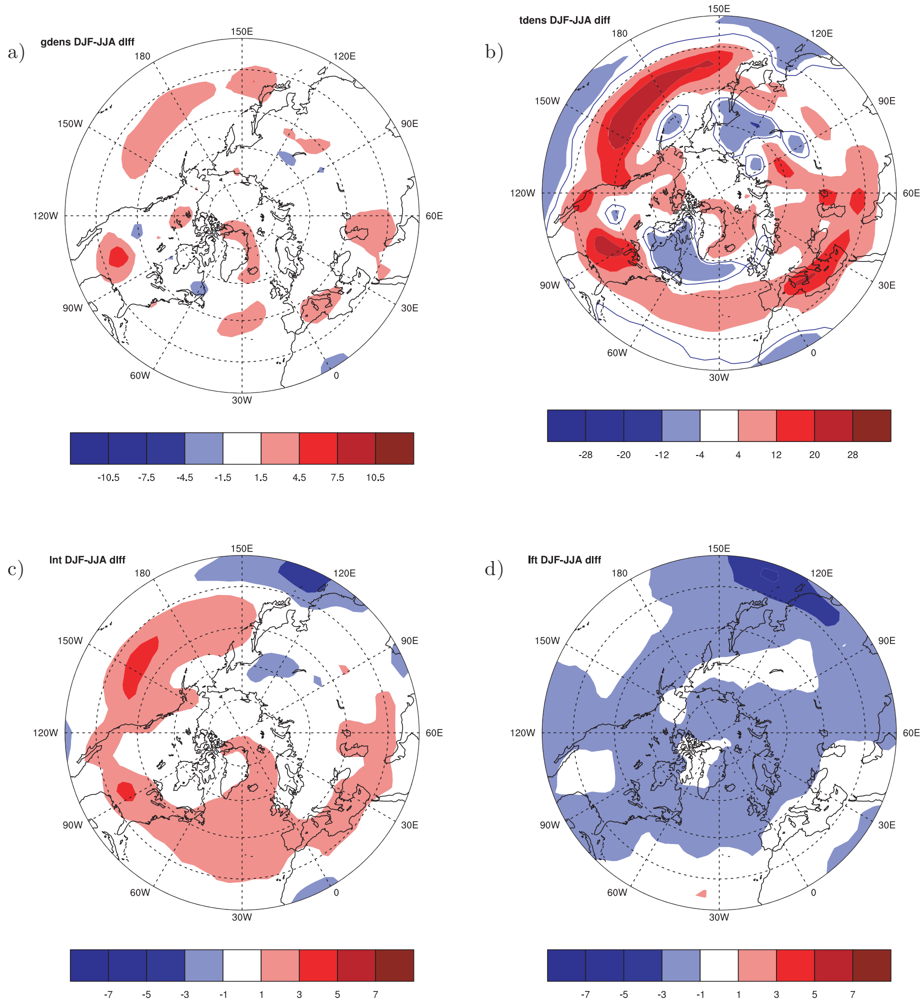

Fig. 3. The difference between the DJF and JJA seasons in the Northern Hemisphere from 1949 to 2002: (a) The genesis density (10^6 km^2 season)$^{-1}$; (b) The track density (10^6 km^2 season)$^{-1}$. To better indicate the preferential eastward lobe into the United Kingdom and southern Scandinavia an extra contour line at -2 storms (10^6 km^2 season)$^{-1}$ was added (i.e. 2 storms (10^6 km^2 season)$^{-1}$ more in the summer); (c) The track intensity (10^{-5} s^{-1}); (d) The mean lifetime (d).

A2—primary track zone and important for assessing impacts on Europe and P—primary track zone for the Pacific. For each of the four storm variables a trend rate, expressed in % per decade based on the 1948 value, was extracted from a linear least squares fit applied to the average of all grid points within the region of interest (A1, A2, P). Table 1 shows the rate of change per decade. The results within these lines are statistically significant at the 95% confidence interval.

Only for region A1 was the trend in cyclogenesis significant—for this region a definite decreasing rate is observed. The track density did not show particularly strong trends in any region.

The feature intensity showed statistically significant changes in all regions, including a definite increase in storm intensity in the Pacific region P. In region A1, although there is a decrease in storm formation activity, there is an increase in intensity. A small yet statistically significant decrease in intensity over Europe is indicated. Only over the Pacific was a strong, statistically significant positive trend in lifetime noted.

3.4. *Relationship to the Northern Annular Mode*

The Northern Annular Mode from Ogi et al. (2004), Fig. 5, is calculated through applying an EOF analysis for each calendar month, which is different from the Northern Annular Mode from Thompson and Wallace (2000). The latter is calculated using a single EOF analysis for all calendar months, which has no seasonal variation and thus underestimates the summer dominant mode. In their breakdown of the NAM into calendar months Ogi et al. (2004) have revealed a pronounced summertime mode. This summertime mode is linked to the winter mode via a lag relationship, that is, when NAM is positive in winter it will also tend to be positive in the summer. The main centre of action for

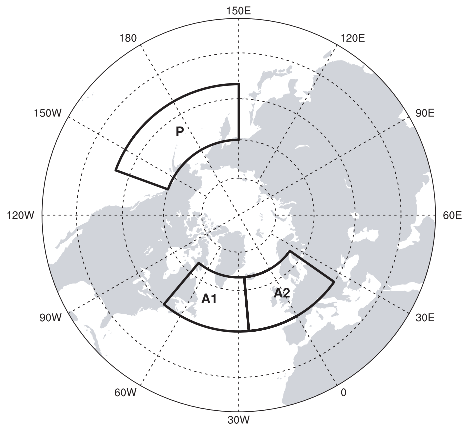

Fig. 4. Regions in the Northern Atlantic and in the Northern Pacific Oceans used to study the storm track variability: Region A1 (70°–25°W, 45°–65°N); Region A2 (25°W–20°E, 45°–65°N) and Region P (150°E–140°W, 40°–60°N).

Table 1. Parameter rate of change per decade: trends of the track variables for two regions in the Atlantic (A1 and A2) and one region in the Pacific (P)

Percentage rate of change per decade since 1948				
Region	Genesis density	Track density	Track intensity	Mean lifetime
A1	**−2.90**	0.31	**1.64**	2.02
A2	1.36	−0.97	**−1.45**	1.29
P	−1.45	1.76	**4.48**	**5.06**

The genesis density trend is statistically significant in region A1. The track density trend is not significant for any of the regions. The track intensity is significant for the three regions, with a negative trend in region A2. The mean lifetime trend is significant in the Pacific Ocean region.
p-values <0.05 are given in bold.

the NAM is located over the Arctic Ocean in the summer, shifting to lie over Greenland during winter. Linkages between storm parameters and the summertime NAM are explored in two ways: first by subsetting storm parameter results by NAM mode, that is, positive or negative (Figs. 6a–d); second, by correlating the NAM index, along with the PDO and NAO indices, to previously defined focus regions (A1, A2 and P, Section 2).

3.4.1. Contrasting NAM positive and negative modes. In order to assess the potential influence of this mode of atmospheric variability on storm track activity, mean values were obtained for subsets of each of the four storm parameters—one subset for positive NAM years (30 in total, hereafter 'NAM+') and one for negative NAM years (25 in total, hereafter 'NAM−')—using NAM monthly values as calculated by Ogi et al. (2004). The differences in these two means, taken as NAM+ minus NAM−, are described below by parameter (Fig. 6).

When the NAM is positive, genesis density is enhanced over the Aleutian islands, the northwestern part of Canada and the USA, between Greenland and Iceland and other areas over the Asian continent. Of interest is a corresponding drop in genesis activity in the central North Atlantic, suggesting a northward shift of genesis activity during positive NAM years (Fig. 6a).

The track density pattern over the Atlantic is opposed to the Pacific one: there are more storms in the Atlantic in NAM+, and more storms in the Pacific in years of NAM−. A dipole pattern is also observed over Northern and Southern Europe. The maximum during NAM+ years is the region from the east coast of Canada up to the Denmark Strait and into the Arctic. Activity is also observed in the vicinity of the Aleutian Islands and the Kara Sea (Fig. 6b).

Even though the number of storms is considerably different from NAM+ to NAM−, the feature intensity is not. Intensity during NAM+ years is higher in the Labrador Sea, the Denmark Strait and in the Arctic Ocean. It is also higher in Asia, southern Europe and southern parts of the Atlantic and the Pacific Oceans. During NAM− years, the intensity is higher over the Beaufort Sea, Great Britain, the eastern part of the Atlantic Ocean, the eastern part of Asia and other parts in the Pacific Ocean

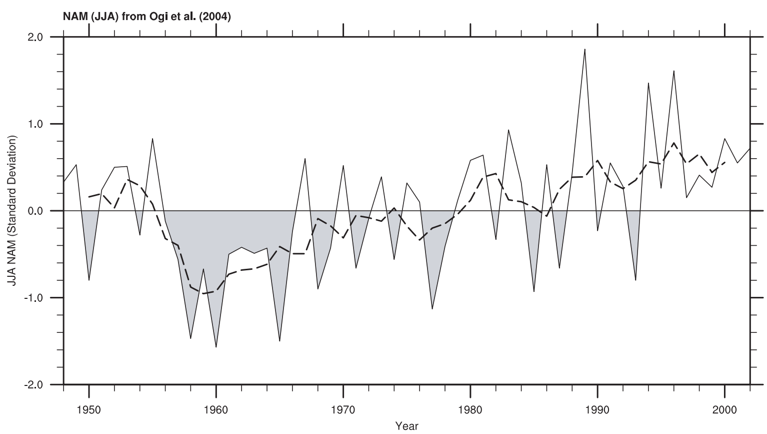

Fig. 5. The Summer (JJA) Northern Annular Mode (NAM) from Ogi et al. (2004). The time-series goes from 1948 to 2002. The dashed line represents a 5-yr running mean.

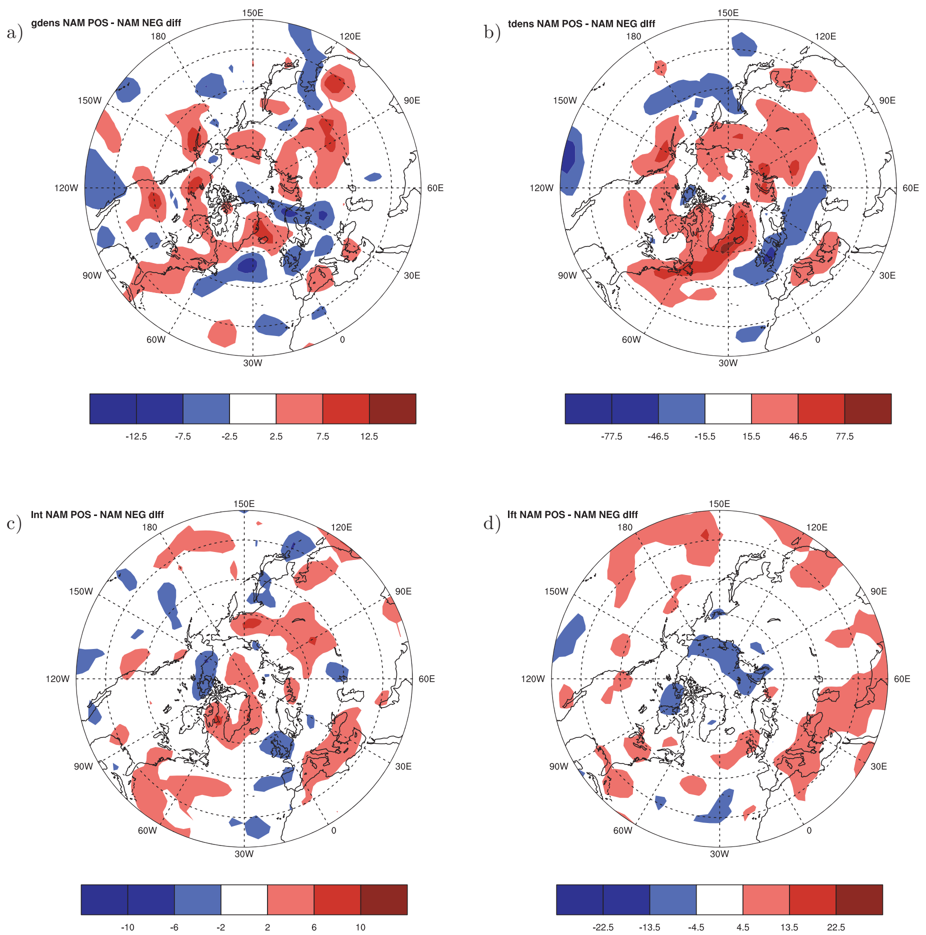

Fig. 6. The storm track climatology of the difference between years when NAM was positive minus years when it was negative: (a) The genesis density (10^6 km^2 season)$^{-1}$; (b) The track density (10^6 km^2 season)$^{-1}$; (c) The track intensity (10^{-5} s^{-1}); (d) The mean lifetime (d).

(Fig. 6c). It must be noted, however, that none of these patterns is very strong.

In the Arctic, summer storms seem to be longer during NAM− years. During NAM+ years, the highest lifetimes are found through the lower latitudes, over the eastern part of the North Atlantic Ocean, parts of the North Pacific, the western coast of the United States and the Great Lakes (Fig. 6d). As with intensity, these patterns are not strong.

3.4.2. Correlating NAM, PDO and NAO to storm track variables in three subregions Three major indices of atmospheric variability (NAM, PDO and NAO) were also correlated to the three focus regions defined for this paper: A1, A2 and P (Tables 2–4).

For the NAM case (Table 2), the highest correlation values with the genesis density are in regions A1 and P. Region A1 shows a negative correlation during years of positive summer NAM (−0.27), whereas the correlation is positive when NAM is negative. The Pacific region shows a similar pattern. However, none of the correlations for the genesis density case are statistically significant.

As for the track density, the highest correlation is in region A1 (0.42) with the summer NAM. Region A2 shows negative correlations of up to −0.34 in years of negative NAM. There is also a negative correlation of −0.25 with NAM. In the Pacific, the highest correlation is during positive NAM years, but this correlation is not statistically significant.

The track intensity shows the highest value in region A1: 0.25 for all NAM years. The lifetime shows higher negative correlations during negative NAM years for regions A1 (−0.37) and A2 (−0.55).

The PDO index (Pacific Decadal Oscillation), which is the leading PC of the monthly sea surface temperature from 20 N in the North Pacific, was similarly correlated with the four storm track variables (Table 3). For the genesis density, the statistically significant correlations are over regions A1 and P. In region A1, the highest correlation (−0.43, p-value = 0.02) is when the PDO is negative (hereafter ‘PDO−’). For all PDO years, the correlation is −0.24 for this region. In the Pacific there is a negative correlation with the PDO of −0.24. There is also a negative correlation of −0.39 with PDO−.

Table 2. The Pearson's product-moment correlation between the track variables in the three regions and the NAM index

	Correlation between NAM (JJA) and the track variables											
Region	Genesis density			Track density			Track intensity			Mean lifetime		
	NAM	NAM+	NAM−	NAM	NAM+	NAM−	NAM	NAM+	NAM−	NAM	NAM+	NAM−
A1	−0.05	−0.27	0.26	**0.42**	0.01	0.14	**0.25**	0.22	0.12	0.10	0.15	**−0.37**
A2	−0.07	0.003	0.15	**−0.25**	0.01	**−0.34**	−0.17	0.01	−0.15	0.05	0.19	**−0.55**
P	0.13	−0.20	0.30	−0.08	−0.25	−0.05	0.02	0.05	−0.03	0.11	0.23	−0.28

Correlations were also performed for NAM+ and NAM− and presented in the table.
p-values <0.1 are given in bold.

Table 3. The Pearson's product moment correlation between the track variables in the three regions studied and the PDO

	Correlation between PDO (JJA) and the track variables											
Region	Genesis density			Track density			Track intensity			Mean lifetime		
	PDO	PDO+	PDO−	PDO	PDO+	PDO−	PDO	PDO+	PDO−	PDO	PDO+	PDO−
A1	**−0.24**	−0.15	**−0.43**	−0.15	−0.18	−0.17	**0.22**	0.20	0.22	**0.25**	0.25	**0.33**
A2	0.03	0.21	−0.03	−0.02	−0.08	0.20	**−0.27**	−0.11	−0.16	0.07	0.07	0.12
P	**−0.24**	−0.26	**−0.39**	−0.07	−0.18	−0.06	**0.35**	0.28	**0.46**	**0.36**	0.29	**0.44**

The correlation when the PDO is positive and negative is also shown. Data obtained from the Joint Institute for the Study of the Atmosphere and Ocean, JISAO, Seattle, USA.
p-values <0.1 are given in bold.

Table 4. The Pearson's product moment correlation between the track variables in the three regions studied and the NAO

	Correlation between NAO (JJA) and the track variables											
Region	Genesis density			Track density			Track intensity			Mean lifetime		
	NAO	NAO+	NAO−	NAO	NAO+	NAO−	NAO	NAO+	NAO−	NAO	NAO+	NAO−
A1	0.02	−0.10	0.06	**0.46**	**0.44**	0.22	0.12	−0.10	0.05	0.17	0.05	−0.12
A2	−0.09	−0.01	0.14	**−0.48**	−0.17	**−0.37**	**−0.34**	−0.23	0.02	0.03	0.12	−0.3
P	0.03	0.013	0.02	**0.23**	0.03	−0.13	**0.25**	0.14	0.11	0.11	0.05	0.09

The correlation when the NAO is positive and negative is also shown. NAO Index Data provided by the Climate Analysis Section, NCAR, Boulder, USA, Hurrell (1995).
p-values <0.1 are given in bold.

The highest correlations for the track density are for region A1, but none of them are statistically significant. The feature intensity in the three regions seem to be correlated to the PDO index. The highest correlation is in the Pacific region during PDO− years: 0.46 (p-value = 0.01). There is also a correlation of 0.35 for all PDO years in the Pacific region. For region A1, a statistically significant correlation is for all PDO years: 0.22. In region A2, the correlation is negative −0.27. The lifetime shows statistically significant correlations for regions A1 and P. The highest correlation value is in the Pacific during PDO− years: 0.44 (p-value = 0.01). There is also a correlation of 0.36 for all PDO years in the Pacific region. Region A1 shows correlations of 0.25 for all PDO years and 0.33 for PDO−.

A correlation with the NAO (PC based) is shown in Table 4 for each track variable There seems to be no statistically significant correlation with the genesis density variable and the NAO.

The track density is well correlated with the NAO for the three regions studied. The highest negative correlation is in region A2, −0.48 (p-value: <0.001). In region A1, the significant correlations found are 0.46 (p-value < 0.001) with the NAO and 0.44

(p-value = 0.01) with the NAO+. A significant correlation of −0.37 (p-value = 0.08) is also found for region A2 with NAO−. In the Pacific the correlation is not so robust: 0.23 (p-value = 0.09).

The only significant correlation coefficients for the feature intensity are in regions A2 and P. In region A2, the correlation is highest: −0.34 (p-value = 0.01) and in region P, the correlation coefficient is 0.25 (p-value = 0.07). There are no statistically significant correlations for the lifetime variable.

4. Discussion

In general, the broadest features of the summertime storm climatology are similar to that exhibited in the winter, that is, activity maxima over the North Atlantic and the North Pacific. Most summer storms are generated downstream from main orographic features or along baroclinic zones, with the Rocky Mountains and the North American eastern seaboard contributing strongly to the North Atlantic storm track.

In the North Atlantic, the corridors followed by summer storms differ in location and form from those observed in winter. In winter, the corridors are more diffuse, extending northward from latitude 40°N, with some concentration between Iceland and Greenland. This is in agreement with results obtained by other work done on the winter season (Murray and Simmonds, 1991; Jones and Simmonds, 1993; Serreze et al., 1993; Serreze, 1995; Barry and Carleton, 2001). The summer storm corridors, on the other hand, are more tightly defined, extending from the east coast of the United States, across the North Atlantic (generally between 50°–60°N), and up on the eastern side of Iceland with a lobe extending east into the vicinity of the United Kingdom/southern Scandinavia. This last feature is an interesting departure from winter, representing a distinct southeastward shift in the storm track as it approaches Europe. This means summer storms will reach Scandinavia and western Europe more often than their winter counterparts.

An important observation is that summer storms are longer lived than winter storms, at 5–7 d versus 4–5 d (Hoskins and Hodges, 2002). In addition, they last longer and tend to be weaker than winter ones. This observation extends upon that made by Zhang et al. (2004) for the Arctic region—the fact that summer storms last longer than winter storms was first observed by Zhang et al. (2004) in a study of storms in the Arctic using the NCEP/NCAR Reanalysis from 1948 to 2002. The tracking algorithm used by Zhang et al. (2004) was an enhanced version of the one by Serreze (1995) and the tracking variable used was the Mean Sea Level Pressure. Another important observation made here about summer storms is the consistency of their long lifespan. This suggests that the lower energy summer systems are dynamically more stable than their higher energy winter counterparts.

The fact that the temperature gradient is weaker in the summer means that there is also less Available Potential Energy (APE), since APE is proportional to the horizontal gradient of temperature. When warm air rises (cooling adiabatically) and cold air sinks (warming adiabatically) APE can be transformed into Kinetic Energy (KE) which will then reduce the temperature gradient (Bluestein, 1992). During summer, this process is much slower because there is less APE available for this conversion, and thus, the smoothing process of the gradient of temperature is slower.

Holton (2004) indicates that observations show that only about 0.5% of the Total Potential Energy (TPE) of the atmosphere is available for conversion, while just 10% of this amount is actually converted to KE. For this reason, Holton (2004) calls the atmosphere a 'rather inefficient heat engine', and here we add that summer storms are even less efficient at this process. Thus, summer storms are less-efficient heat engines, which gives rise to their longevity because they take longer to equalize the temperature gradient on which they depend. Although weaker summer systems do not tend to cause dramatic, high-wind events their longevity has important implications for precipitation—slow-moving, long-lived storms are more likely to cause flooding events. In this regard, of particular note in the results presented here is that a trend towards increased storm durations over Europe is indicated.

Other results identified regionally significant trends in various parameters over the North Pacific, southern Europe, northeastern parts of Canada, parts of the North Atlantic and other parts in the Northern Hemisphere. These could represent a manifestation of a changing climate in higher latitudes. It is also possible, however, that these trends in storm parameters could also be the result forcing due to low-frequency variability of the large-scale flow, as represented by correlations with major indices of atmospheric variability, including the NAM, the PDO and the NAO. In the latter case, the extent to which storm parameter trends are a manifestation of climate change depends upon the extent to which trends in the variability indices are linked to climate change.

The high cyclogenesis and storm values for the summer found over the Hudson Bay may be due to the fact that there is more open water compared to the winter season, and the more northerly position of the polar front baroclinic zone. In addition, higher temperatures in the summer would promote evaporation, enhancing cyclogenesis potential. In a paper about summer and winter storms in the Arctic, Serreze (1995) pointed out that during summer '. . .local diabatic heating associated with open water areas within the ice cover can be significant, and in some cases might contribute to rejuvenation.' Serreze (1995) did not, however, identify the cyclogenesis region from western Hudson Bay extending into northern Baffin Island. He mentions that these features were observed by Whittaker and Horn (1984), but that this region was '. . .not observed in the present data,' that is, in his data set. Serreze (1995) developed his own tracking algorithm using MSLP. An MSLP-based method is unlikely to find the Hudson Bay cyclogenesis region because the vorticity field detects features much earlier than the MSLP field.

Findings in all four storm track parameters accentuate the substantial activity in the Arctic. This also echoes findings in Serreze (1995), which suggests that the increased high latitude cyclonic activity during summer is related to the development of a seasonal Arctic frontal zone that is separate from the polar front. Serreze (1995) also suggests that more open water areas in high latitudes can contribute significantly to rejuvenation.

Hoskins and Hodges (2002) mention that most variables give the Atlantic storm track to be stronger than the Pacific. However, the 850-hPa Z, V and vorticity make them equal. These results are for the winter season. In our study, we find the Atlantic storm track to be slightly weaker (Fig. 1c) but with higher number of storms (Fig. 1b).

Finally, there is a connection between summer storm tracks and the summer NAM, by Ogi et al. (2004). The most striking feature is that the storms are shifted northwards into the Denmark Strait during years of positive NAM in the North Atlantic. However, there are more storms over Great Britain and southern Scandinavia during years of negative NAM (Fig. 6b). Overall, results suggest that the NAM affects the position, but not the strength, of the major baroclinic zones and hence is correlating with storm track but not intensity. There is also a connection between the PDO index, which is related to the sea surface temperature, and all storm parameters except track density. The NAO is also connected to the storm tracks in the region studied, especially the track density and feature intensity variables.

4. Acknowledgments

This work has been done with support from the RegClim project (http://regclim.met.no/) funded by the Research Council of Norway. It has also received support from the Norwegian Super Computing Committee (TRU) through a grant of computing time on an IBM Regatta computer at Parallab, University of Bergen.

We acknowledge the Bjerknes Centre for Climate Research (BCCR, Bergen, Norway) and the International Arctic Research Center (IARC, Fairbanks, AK, USA) for the technical support given under the research. We would also like to thank Dr. John Walsh for the invaluable comments and discussions on this paper.

References

Anderson, D., Hodges, K. I. and Hoskins, B. J. 2003. Sensitivity of feature-based analysis methods of storm tracks to the form of background field removal. *Mon. Wea. Rev.* **131**, 565–573.

Barry, R. and Carleton, A. 2001. *Synoptic and Dynamic Climatology*. Routledge, New York.

Bell, G. D. and Bosart, L. F. 1989. A 15-year climatology of northern hemisphere 500 mb closed cyclone and anticyclone centers. *Mon. Wea. Rev.* **117**, 2142–2164.

Blackmon, M. L. 1976. A climatological spectral study of the 500 mb geopotential height of the Northern Hemisphere. *J. Atmos. Sci.* **33**, 1607–1623.

Blackmon, M. L., Wallace, J. M., Lau, N. C. and Mullen, S. J. 1977. An observational study of the northern hemisphere wintertime circulation. *J. Atmos. Sci.* **34**, 1040–1053.

Bluestein, H. B. 1992. *Synoptic-Dynamic Meteorology in Midlatitudes*. **I**, Oxford University Press, New York.

Bluestein, H. B. 1993. *Synoptic-Dynamic Meteorology in Midlatitudes*. **II**, Oxford University Press, New York.

Byrkjedal, Ø. 2002. *Storm Tracks with Different Ice Cover in the Labrador Sea (in Norwegian)*, Master's Thesis. Universitetet i Bergen, Bergen.

Cai, M. and van der Dool, H. 1991. Low-frequency waves and traveling storm tracks. I. Barotropic component. *J. Atmos. Sci.* **48**, 1420–1436.

Chang, E. K. M. 2004. Are the Northern Hemisphere winter storm tracks significantly correlated? *J. Climate* **17**, 4230–4244.

Chang, E. K. M. and Orlanski, I. 1993. On the dynamics of a storm track. *J. Atmos. Sci.* **50**, 999–1015.

Chang, E. K. M. and Fu, Y. 2002. Interdecadal variations in Northern Hemisphere winter storm track intensity. *J. Climate* **15**, 642–658.

Chang, E. K. M., Lee, S. and Swanson, K. L. 2002. Storm tracks dynamics. *J. Climate* **15**(16), 2163–2183.

Graham, N. and Diaz, H. 2001. Evidence for intensification of North Pacific winter cyclones since 1948. *B. Am. Meteorol. Soc.* **82**(9), 1869–1893.

Gulev, S., Zolina, O. and Grigoriev, S. 2001. Extratropical cyclone variability in the Northern Hemisphere winter from the NCEP/NCAR reanalysis data. *Clim. Dyn.* **17**, 795–809.

Hodges, K. I. 1994. A general method for tracking analysis and its application to meteorological data. *Mon. Wea. Rev.* **122**, 2573–2586.

Hodges, K. I. 1995. Feature tracking on the unit sphere. *Mon. Wea. Rev.* **123**, 3458–3465.

Hodges, K. I. 1996. Spherical nonparametric estimates applied to the UGAMP model integration for AMIP. *Mon. Wea. Rev.* **124**, 2914–2932.

Hodges, K. I. 1999. Adaptive constraints for feature tracking. *Mon. Wea. Rev.* **127**, 1362–1373.

Hodges, K. I., Hoskins, B. J., Boyle, J. and Thorncroft, C. 2003. A comparison of recent re-analysis data sets using objective feature tracking: storm tracks and tropical easterly waves. *Mon. Wea. Rev.* **131**, 2012–2037.

Holton, J. 2004. *An Introduction to Dynamic Meteorology*. 4th Edition, International Geophysics Series. Elsevier Academic Press, London.

Hoskins, B. and Hodges, K. I. 2002. New perspectives on the Northern Hemisphere winter storm-tracks. *J. Atmos. Sci.* **59**, 1041–1061.

Hurrell, J. W. 1995. Decadal trends in the north atlantic oscillation regional temperatures and precipitation. *Science* **269**, 676–679.

Jones, D. and Simmonds, I. 1993. A climatology of southern hemisphere extratropical cyclones. *Clim. Dyn.* **9**, 131–145.

Kalnay, E., Kanamitsu, M., Kistler, R., Collins, W., Deaven, D., and coauthors. 1996. The NCEP/NCAR 40-Year Reanalysis Project. *Bull. Amer. Meteor. Soc.* **77**, 437–471.

Keegan, T. J. 1958. Arctic synoptic activity in winter. *J. Atmos. Sci.* **15**, 513–521.

Kistler, R., Kalney, E., Collins, W., Saha, S., White, G., and co-authors. 2001. The NCEP-NCAR 50-year reanalysis: monthly means CD-ROM and documentation. *B. Am. Meteorol. Soc.* **82**, 247–267.

König, W., Sausen, R. and Sielmann, F. 1993. Objective identification of cyclones in GCM simulations. *J. Climate* **6**, 2217–2231.

Lamb, H. 1991. *Historic Storms of the North Sea, British Isles and Northwest Europe*. The Press Syndicate of the University of Cambridge, Cambridge.

Lambert, S. J. 1996. Intense extratropical Northern Hemisphere winter cyclone events: 1899–1991. *J. Geophys. Res.* **101**(D16), 21319–21326.

Leonard, S. R., Turner, J. and Van Der Wal, A. 1999. An assessment of three automated depression tracking schemes. *Meteorol. Appl.* **6**, 173–183.

Lydolph, P. E. 1977. *Climates of the Soviet Union* Volume 7, World Survey of Climatology, Elsevier Scientific Publishing Company, New York.

Mailier, P. J., Stephenson, D. B., Ferro, C. A. T. and Hodges, K. I. 2006. Serial clustering of extratropical cyclones. *Mon. Wea. Rev.* **134**, 2224–2240.

Murray, R. and Simmonds, I. 1991. A numerical scheme for tracking cyclone centres from digital data. Part I: development and operation of the scheme. *Aust. Met. Mag.* **39**, 155–166.

Norris, J. R. 2000. Interannual and interdecadal variability in the storm track, cloudiness, and sea surface temperature over the summertime North Pacific. *J. Clim.* **13**, 422–430.

Ogi, M., Yamazaki, K. and Tachibana, Y. 2004. The summertime annular mode in the Northern Hemisphere and its linkage to the winter mode. *J. Geophys. Res.* **109**, D20114, doi:10.1029/2004JD004514.

Pinto, J. G., Spangehl, T., Ulbrich, U. and Speth, P. 2005. Sensitivities of a cyclone detection and tracking algorithm: individual tracks and climatology. *Meteorol. Z.* **14**(6), 823–838.

Reed, R. J. and Kunkel, B. A. 1960. The arctic circulation in summer. *J. Atmos. Sci.* **17**, 489–506.

Reitan, C. H. 1974. Frequencies of cyclones and cyclogenesis for North America, 1951–1970. *Mon. Wea. Rev.* **102**, 861–867.

Salari, I. and Sethi, K. 1990. Feature point correspondence in the presence of occlusion. *IEEE Trans. PAMI* **12**(1), 87–91.

Serreze, M. 1995. Climatological Aspects of cyclone development and decay in the arctic. *Atmos.-Ocean* **33**, 1–23.

Serreze, M., Box, J., Barry, R. and Walsh, J. 1993. Characteristics of arctic synoptic activity. *Met. Atmos. Phys.* **51**, 147–164.

Serreze, M., Carse, F. and Barry, R. 1997. Icelandic low cyclone activity: climatological features, linkages with the NAO, and relationships with recent changes in the Northern Hemisphere circulation. *J. Climate* **10**, 453–464.

Serreze, M., Lynch, A. H. and Clark, M. P. 2000. The Arctic frontal zone as seen in the NCEP-NCAR reanalysis. *J. Climate* **14**, 1550–1567.

Simmonds, I. and Keay, K. 2000. Mean Southern Hemisphere extratropical cyclone behavior in the 40-year NCEP-NCAR reanalysis. *J. Climate* **13**, 873–885.

Simmonds, I. and Keay, K. 2002. Surface fluxes of momentum and mechanical energy over the North Pacific and North Atlantic oceans. *Meteor. Atmos. Phys.* **80**(1), 1–18.

Simmonds, I., Murray, R. J. and Leighton, R. M. 1999. A refinement of cyclone tracking methods with data from FROST. *Aust. Met. Mag.*, Spec. Ed., 35–49.

Simmonds, I., Keay, K. and Lim, E. P. 2003. Synoptic activity in the seas around Antarctica. *Mon. Wea. Rev.* **131**, 272–288.

Sinclair, M. R. 1994. An objective cyclone climatology for the Southern Hemisphere. *Mon. Wea. Rev.* **122**, 2239–2256.

Sinclair, M. R. 1995. A climatology of cyclogenesis for the Southern Hemisphere. *Mon. Wea. Rev.* **123**, 1601–1619.

Sorteberg, A. and Walsh, J. 2008. Seasonal cyclone variablity at 70 N and its impact on moisture transport into the Arctic. *Tellus* **60A**, 10.1111/j.1600-0870.2008.00314.x.

Sorteberg, A., Kvamstø, N. G. and Byrkjedal, O. 2005. Wintertime nordic seas cyclone variability and its impact on oceanic volume transports into the Nordic Seas. In: *The Nordic Seas, An Integrated Perspective* Volume 158 (eds H. Drange, T. Dokken, T. Furevik, R. Gerdes and W. Berger), Am. Geophys. Union, Washington DC, 137–156.

Terry, J. and Atlas, R. 1996. Objective cyclone tracking and its applications to ERS-1 scatterometer forecast impact studies. In: *Proceedings of the Fifteenth Conference on Weather Analysis and Forecasting Conference*, Norfolk, VA, *Amer. Meteor. Soc.*, 146–149.

Thompson, D. W. J. and Wallace, J. M. 2000. Annular modes in the extratropical circulation. Part I: month-to-month variability. *J. Climate* **13**, 1000–1016.

Turner, J., Marshall, G. J. and Lachlan-Cope, T. A. 1998. Analysis of synoptic-scale low pressure systems within the Antarctic peninsula sector of the circumpolar trough. *Int. J. Climatol.* **18**(3), 253–280.

Whittaker, L. and Horn, L. 1981. Geographical and seasonal distribution of north american cyclogenesis, 1958–1977. *Mon. Wea. Rev.* **109**, 2312–2322.

Whittaker, L. and Horn, L. 1984. Northern Hemisphere extratropical cyclone activity for four mid-season months. *J. Climatol.* **4**(3), 297–310.

Zhang, X., Walsh, J., Bhatt, U. and Ikeda, M. 2004. Climatology and interannual variability of arctic cyclone activity: 1948–2002. *J. Climate* **17**, 2300–2317.

Zhang, Y., Wallace, J. M. and Battisti, D. S. 1997. ENSO-like interdecadal variability: 1900–93. *J. Climate* **10**, 1004–1020.

Zishka, K. M. and Smith, P. J. 1980. The climatology of cyclones and anticyclones over North America and surrounding ocean environments for January and July, 1950–1977. *Mon. Wea. Rev.* **108**, 387–401.

Zolina, O. and Gulev, S. K. 2002. Improving the accuracy of mapping cyclone numbers and frequencies. *Mon. Wea. Rev.* **130**, 748–759.